
Postprint Version

C.V. Brown, G.G. Wells, M.I. Newton and G. McHale, *Voltage-programmable liquid optical interface*, Nature Photonics 3 (7) (2009) 403-405; DOI: 10.1038/nphoton.2009.99.

VOLTAGE-PROGRAMMABLE LIQUID OPTICAL INTERFACE

C.V. Brown*, G.G. Wells, M.I. Newton and G. McHale

School of Science and Technology, Nottingham Trent University,
Clifton Lane, Nottingham NG11 8NS, UK

There has been intense recent interest in photonic devices based on microfluidics that include displays [1,2] and refractive tunable microlenses and optical beamsteerers [3-5] that work using the principle of electrowetting [6,7]. Here we report a novel approach to optical devices in which static wrinkles are produced at the surface of a thin film of oil as a result of dielectrophoretic forces [8-10]. We have demonstrated this voltage programmable surface wrinkling effect with periodic devices with pitch lengths of between 20 µm and 240 µm and with response times of less than 40 µs. By careful choice of oils, it is possible to optimise either for high amplitude sinusoidal wrinkles at micrometer-scale pitches or for more complex non-sinusoidal profiles with higher Fourier components at the longer pitches. This provides the possibility for rapidly responsive voltage programmable polarisation insensitive transmission and reflection diffraction devices and for arbitrary surface profile optical devices.

* E-mail: carl.brown@ntu.ac.uk, Tel: 44 115 8483184

The structure of the device is shown in figure 1. The side view, in figure 1(a), shows the glass substrate coated with patterned gold/titanium conducting electrodes, on which there is a thin solid dielectric layer (either photoresist or a dielectric stack), upon which is coated a thin layer of oil. The electrodes were arranged as an array of stripes parallel to the *y* direction in the *xy* plane. This geometry allowed every other electrode to be electrically connected as shown in the plan view in figure 1(b).

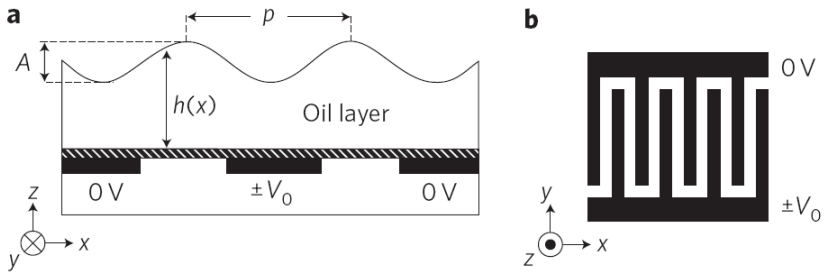

Figure 1 (a) Side view of the structure of the device. A thin layer of oil coats a dielectric layer (shown cross hatched) which has been deposited onto a glass substrate containing an array of gold/titanium interdigitated striped electrodes (shown by the black electrodes). (b) Plan view of the interdigitated electrode geometry.

The electrically induced wrinkling at the oil surface will be considered first for a device with an electrode pitch of p = 80 μm. When a small volume (0.1 μL) of 1-decanol was initially dispensed onto the device it formed a spherical cap with a contact angle of 5°. Every other stripe in the electrode array was biased with an A.C. voltage with r.m.s. magnitude V_O and the inter-digitated stripes between them were earthed, as shown in figure 1. This creates a periodic electric field profile in the plane of the oil layer which is highly non-uniform. A polarisable dielectric material in a region containing non-uniform electric fields experiences a force, known as a dielectrophoretic force, in the direction of the increase in magnitude of the electric field [8-10]. When the r.m.s. electrode voltage was greater than V_O = 20 Volts the dielectrophoretic forces spread the oil into a thin film with a uniform thickness, $\bar{h}$ = 12 μm, across the area covered by the electrodes.

Increasing the voltage between neighbouring electrodes gave rise to a periodic undulation at the surface of the oil. The period of the wrinkle was equal to the electrode pitch, 80 μm, and the peaks and troughs of the wrinkle lay parallel to the electrode fingers along the *y*-direction. This undulation arises because the highest electric field gradients occur in the gaps between the electrodes and so the dielectrophoretic forces in these regions cause the oil to collect there preferentially. The interdigitated electrode geometry is commonly used in biological particle manipulation [9, 11] but dielectrophoretic actuation in fluids has previously been limited to nanodroplet formation and lab-on-a-chip applications [12].

The wrinkle at the oil/air interface and the associated periodic variation in the optical path for light travelling through the film has been directly visualised using a Mach-Zehnder interferometer [13]. The device was illuminated in transmission with He-Ne laser light at a wavelength of 633 nm. One of the mirrors of the interferometer was tilted to produce parallel intensity interference fringes localised at the position of the oil layer. The individual interference fringes

were parallel to the x direction and a periodic change in the oil thickness $h(x)$ causes a directly proportionate periodic shift of the fringes in the y direction. The interferograms (a) and (b), inset into figure 2, show the fringe patterns when voltages of V_O = 80 V and V_O = 160 V (20 kHz A.C.) respectively were applied between adjacent in-plane electrodes.

Knowledge of the refractive index of the oil (n_{oil} = 1.438 for 1-decanol [14]) allowed the peak-to-peak amplitude A of the wrinkle at the oil/water interface to be calculated directly from the interferometer fringe patterns. The results are shown by the filled circles in figure 2, where the square of the r.m.s. amplitude V_O of the applied voltage is plotted as the abcissae. The solid line shows the linear regression fit to the data: $A = (5{\cdot}107 \times 10^{-5})\, V_o^2 + 0{\cdot}118$ in *micrometers*.

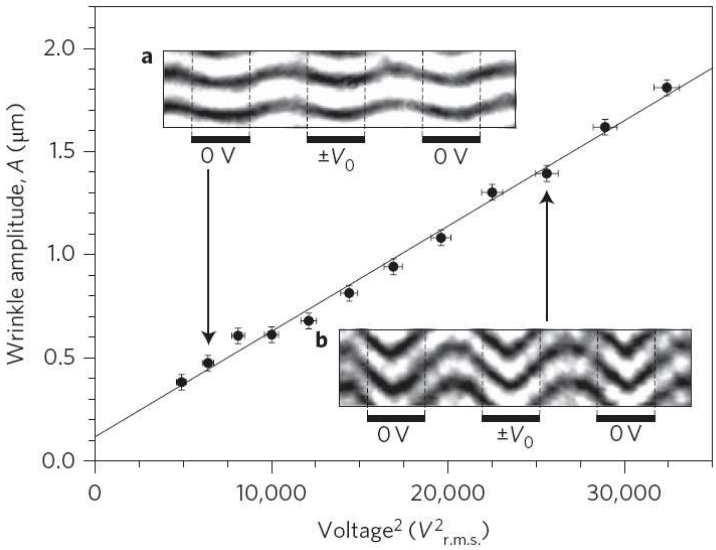

Figure 2 Periodic displacements of tilt fringes at a wavelength of 633 nm (0.61 mW cm^{-2} at device) in a Mach-Zehnder interferometer (a) and (b), shown inset. These fringe patterns were produced by a layer of 1-decanol oil coating a device with a dielectric stack of thickness 1.13 μm (supplementary information) with voltages of 80 V and 160 V (r.m.s. 20 kHz A.C.) respectively. The electrode (and wrinkle) pitch was 80 μm. The peak to peak amplitude A of the wrinkle at the oil/air interface, obtained from the interferometer fringe patterns, is plotted against the square of the A.C. voltage, V_O^2.

Under an applied periodic potential the appearance of the wrinkle at the oil/air interface decreases the dielectric energy of the system, but this in turn causes an increase in the area of the oil/water interface. The interfacial surface tension provides the restorative force which resists the undulation deformation on the spread oil film. The observed dependence on the square of the voltage is reproduced by a simple calculation using the following approximations: (i) the wrinkle amplitude is small ($A << p$); (ii) the periodic potential profile due to the electrodes, $V(x, y)$, is described by a Fourier series expansion to second order only; and (iii) the potential profile is unperturbed by the presence of the oil/air interface. Equating and minimising the sum of the electrostatic and the surface tension energies with respect to the peak-to-peak amplitude A of the wrinkle yields equation 1.

$$A = \left[\frac{16\varepsilon_O}{3\gamma\pi^4} (\varepsilon_{oil} - \varepsilon_{air}) \exp\left(-\frac{4\pi\bar{h}}{p} \right) \right] V_O^2 \qquad (1)$$

This reproduces the intuitive result that, at a particular voltage, higher wrinkle amplitudes will result from using oil with a higher dielectric constant and a lower surface tension. Substituting the values from the linear regression fit to the data in figure 2 and the values of $\varepsilon_{oil} = 8{\cdot}1$ and $\gamma = 28{\cdot}4$ mN m^{-1} [14] for the dielectric constant and surface tension respectively of 1-decanol into equation 1 yields $\bar{h} = 5.5$ μm. This is the correct order of magnitude but lower than the average thickness of $\bar{h} = 12$ μm estimated from the fringe pattern at the edge of the spread film (supplementary information).

The switching speed was measured by monitoring the time dependent intensity of the reflection mode first order diffraction peak in response to a sudden change in the amplitude of the voltage V_O. The device was illuminated in reflection with laser light at a wavelength of 543 nm and the applied voltage (20 kHz A.C. square-wave) was discontinuously switched between a low value, $V_O = 10$ V, and a high value every 5 ms. The low value was just sufficient to maintain the uniformity of the oil coating. The high value of the voltage was adjusted to achieve a peak in the intensity of the first diffracted order for each particular oil film thickness. For the 3 different thicknesses, $\bar{h} = 20$ μm, 18 μm, and 14 μm the r.m.s. amplitudes of the high voltages were $V_O =$ 93 V, 90 V, and 86 V respectively. From simultaneous transmission measurements of the high voltage fringe displacements on the Mach-Zehnder interferometer this was found to correspond to a wrinkle of amplitude $A = 0.36$ μm for all cases. Data is shown in figure 3 for the low to high voltage transition labelled switch, and for the high to low voltage transition labelled relax. The times for the intensity to change from the value at 0 μs to 90% of the difference between the initial and asymptotic intensities were 35 μs, 40 μs, 49 μs (switching) and 79 μs, 89 μs, 108 μs (relaxing) for $\bar{h} = 20$ μm, 18 μm, and 14 μm respectively.

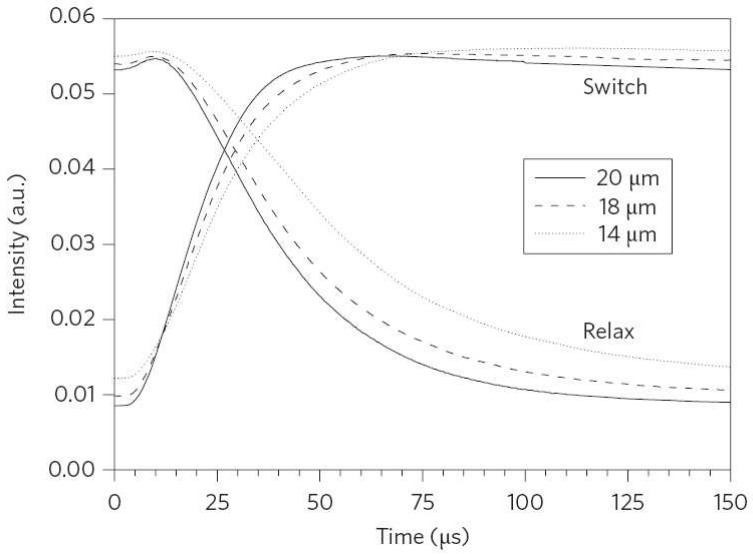

Figure 3 The transient response of the intensity of the reflection mode first diffracted order at 543 nm (0.08 W cm^{-2}) as a function of time after a wrinkle of amplitude $A = 0.36$ μm at the surface of 1-decanol was turned on ("Switch") or off ("Relax") at time 0 μsec. Measurements are shown for oil layers of 3 different thicknesses coating the same device that was used for figure 2 above for which the pitch was $p = 80$ μm.

An amplitude programmable phase diffraction grating [15] has been demonstrated in transmission mode using wrinkles with a shorter pitch of p = 20 μm in a film of 1-decanol oil having average thickness $\bar{h}$ = 3 μm. Figure 4 shows the intensities of the zero, first and second order peaks due to the diffraction of light at 543 nm transmitted through the film with its periodic surface wrinkle as a function of the voltage V_O (20 kHz A.C.) (see also the supplementary information). The ratio of the peak intensity in the first order to the zero order peak intensity at low voltage is 32.6%. This is close to the value of 33.8% which would be predicted by the Fraunhofer approximation for a "thin sinusoidal phase grating" [16].

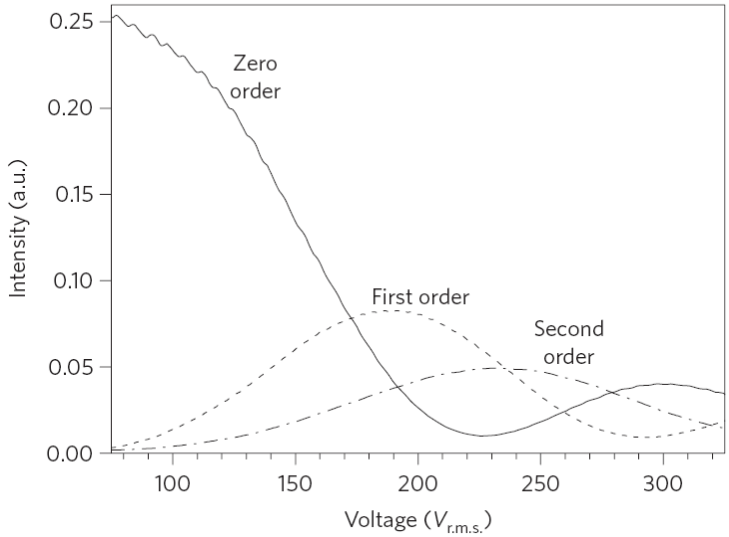

Figure 4 The intensities of the transmitted diffracted orders at 543 nm (0.08 W cm^{-2}) for a film of 1-decanol with average thickness $\bar{h}$ = 3 μm as a function of the magnitude of the voltage (20 kHz A.C.) applied between adjacent in-plane electrodes. The orders were observed at angles of 0º (zero), 1.56º (+1) and 3.11º (+2). For this device the dielectric layer was 2 μm thick and was fabricated from SU-8 photoresist (supplementary information) and the electrode pitch was p = 20 μm, which also corresponded to the wrinkle pitch.

Still shorter pitches of microns or lower appear feasible, but there are technological challenges in creating a sufficiently thin film of oil. Still higher diffraction efficiencies may be possible by making the fluid surface (rather than the substrate) fully reflective [17,18]. It is also possible that the surface wrinkle could be produced at the interface between two density matched liquids, e.g. a high refractive index oil and water, in an encapsulated device which can be used in any orientation [3] (supplementary information).

Figure 5 shows oil film surface shapes that are more interesting than the simple sinusoid-shaped profiles that have been discussed above. Each of the solid lines shows an individual surface profile that has been created for a particular voltage (represented using different colours) and for a particular average oil film thickness (shown by the horizontal dotted line on which it lies). By using oil with a lower dielectric constant (hexadecane, ε_{oil} = 2.05), combined with a longer electrode pitch (p = 240 μm) it has been possible to program non-sinusoidal profiles, and so switch on other Fourier components with higher spatial frequencies. These higher Fourier

components are most prominent at the lowest film thickness, $\bar{h}$ = 6.0 µm, where the surface of the oil film lies closer to the highly non-uniform fringing electric fields at the electrode edges.

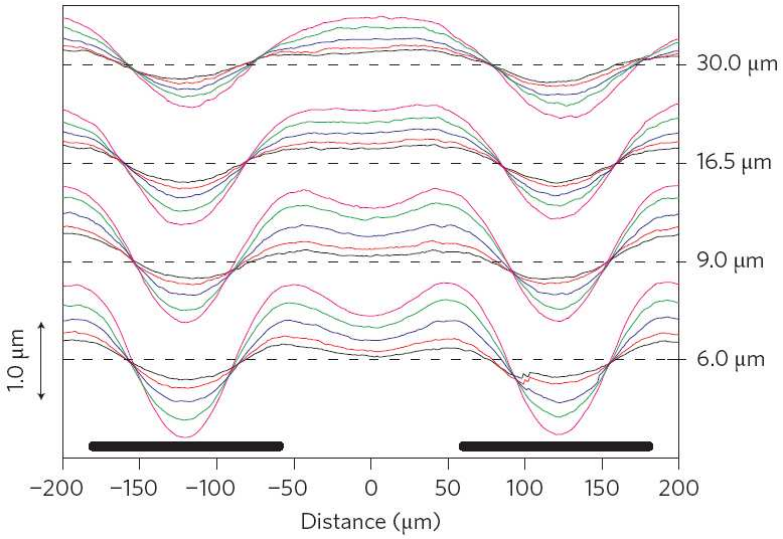

Figure 5 Profiles at a hexadecane oil/air interface that have been created by the action of a non-uniform electric field profile. The profiles were measured using a Mach-Zehnder interferometer (633 nm and 0.61 mW cm^{-2} at the device). Oil films with 4 different thicknesses were used, $\bar{h}$ = 6.0 µm, 9.0 µm, 16.5 µm, and 30.0µm, as indicated by the dotted lines. At each different thickness the profiles are obtained with different applied voltages are shown by the solid lines in different colours: $V_{r.m.s.}$ = 275 V (black), 325 V (red), 400 V (blue), 475 V (green) and 550 V (magenta). For this device the dielectric layer was 2 µm thick and was fabricated from SU-8 photoresist (supplementary information) and the electrode pitch was p = 240 µm, which also corresponded to the wrinkle pitch. The positions of the electrodes are shown by the black lines at the bottom of the figure. The vertical scale is the same for each profile but the

In conclusion, we have presented a new and potentially versatile concept of using dielectrophoretic forces to create fluid based optical switching devices. As an example photonic device application we have demonstrated a switchable phase diffraction grating where the intensity modulation of the undeviated zero order, as well as the diffracted orders, are intrinsically polarisation insensitive; the zero and first order intensities can be fully modulated at speeds of below 40 µs. The voltage programmable optical effect uses a straightforward device structure and is static, reproducible, and stable [19-21] when switched on. This combination of properties in a single device is significant compared with existing technologies based on, for example, birefringent liquid crystals [22,23], electro-optic or acousto-optic modulators [24,25], or deformable polymer layers [26]. Our further demonstration of more complex non-sinusoidal surface wrinkle profiles suggests the possibility of producing aperiodic or arbitrary surface profiles using independently addressable electrodes for application in 2-dimensional spatial light modulator arrays.

Supplementary Information

Videos showing the modulation of the diffraction pattern in response to a slowly ramping voltage (i) in transmission mode using the 20 micron pitch, and (ii) in reflection mode using the 80

micron pitch are available as supplementary information. The supplementary information also provides additional experimental details and discussion of eq. (1).

References

[1] Hayes, R. A. & Feenstra, B. J. Video-speed electronic paper based on electrowetting. *Nature* **425**, 383-385 (2003).

[2] Heikenfeld, J. & Steckl, A.J. High-transmission electrowetting light valves. *Appl. Phys. Lett.* **86**, 151121-151123 (2005).

[3] Berge, B. & Peseux, J. Variable focal lens controlled by an external voltage: An application of electrowetting. *Euro. Phys. J. E* **3**, 159-163 (2000).

[4] Kuiper, S. & Hendriks, B. H. W. Variable-focus liquid lens for miniature cameras. *Appl. Phys. Lett.* **85**, 1128-1130 (2004).

[5] Smith, N.R., Abeysinghe, D.C., Haus, J.W. & Heikenfeld, J. Agile wide-angle beam steering with electrowetting microprisms. *Opt. Exp.* **14**, 6557-6563 (2006).

[6] de Gennes, P. G. Wetting: statics and dynamics. *Rev. Mod. Phys.* **57**, 827-862 (1985).

[7] Mugele, F. & Baret, J. C. Electrowetting: From basics to applications. *J. Phys. Condens. Matter* **17**, R705-R774 (2005).

[8] Pellat, H. Mésure de la force agissant sur les diélectriques liquides non électrisés placés dans un champ électrique. *C. R. Acad. Sci. Paris* **119**, 691-694 (1895).

[9] Pohl, H.A. Dielectrophoresis: *The behaviour of neutral matter in non-uniform electric fields*. (Cambridge Monographs on Physics: Cambridge University Press, Cambridge, 1978).

[10] Lorrain, P. & Corson, D.R. *Electromagnetic Fields and Waves*. 2nd ed. (W.H. Freeman, San Francisco, CA, 1970).

[11] Pethig, R. Using Inhomogeneous AC Electrical Fields to Separate and Manipulate Cells, *Crit. Rev. Biotech.* **16**, 331-348 (1996).

[12] Jones, T.B., Gunjii, M., Washizu, M. & Feldman, M.J. Dielectrophoretic liquid actuation and nanodroplet formation. J. Appl. Phys. **89**, 1441-1448 (2001).

[13] Born, M. & Wolf, E. *Principles of optics*. 7th ed. (Cambridge University Press, Cambridge, 2005).

[14] Knovel Critical Tables (2nd Edition). Knovel, 2003.

[15] Hutley, M.C. *Diffraction Gratings*. (Academic Press, London, 1982).

[16] Goodman, J.W. *Introduction to Fourier Optics*. 2nd ed. (McGraw-Hill, New York, 1996).

[17] Girault, H.H. *Nature Materials* **5**, 851 - 852 (01 Nov 2006).

[18] Bucaro, M.A., Kolodner, P.R., Taylor, J.A., Sidorenko, A., Aizenberg, J., & Krupenkin, T.N., Tunable Liquid Optics: Electrowetting-Controlled Liquid Mirrors Based on Self-Assembled Janus Tiles. *Langmuir* **25**, 3876–3879 (2009).

[19] Herminghaus, S. Dynamical instability of thin liquid films between conducting media. *Phys. Rev. Lett.* **83**, 2359-2361 (1999).

[20] Schäffer, E., Thurn-Albrecht, T., Russell, T. P. & Steiner, U. Electrically induced structure formation and pattern transfer. *Nature* **403**, 874 (2000).

[21] Staicu A. & F. Mugele, F. Electrowetting-induced oil film entrapment and instability. *Phys. Rev. Lett.* **97**, 167801-167804 (2006).

[22] Komanduri, R.K., Chulwoo, O., & Escuti, M.J. Reflective liquid crystal polarization gratings with high efficiency and small pitch. *Liquid Crystals XII*. Edited by Khoo, Iam Choon. *Proc. SPIE*, **7050**, 70500J-70500J-10 (2008).

[23] De La Tocnaye, J.L.D. Engineering liquid crystals for optimal uses in optical communication systems, *Liquid Crystals* **31**, 241-269 (2004).
[24] Eldada, L. Optical communication components. *Rev. Sci. Instr.* **75**, 575- 593 (2004).
[25] Mias, S. & Camon, H. A review of active optical devices: I. Amplitude modulation. *J. Micromech. Microengin.* **18**, 083001 (2008).
[26] Bowden, N., Brittain, S., Evans, A.G., Hutchinson, J.W., & Whitesides, G.M. Spontaneous formation of ordered structures in thin films of metals supported on an elastomeric polymer. *Nature* **393**, 146-149 (1998).

Acknowledgements
The authors gratefully acknowledge J. Fyson at Kodak (European Research) Ltd and N.J. Shirtcliffe and C.L. Trabi at Nottingham Trent University for fruitful discussions. GW gratefully acknowledges The EPSRC/DTI COMIT Faraday Partnership and Kodak (European Research) Ltd. for funding

Additional Information for Postprint
The full supplementary information is available at:
http://www.nature.com/nphoton/journal/v3/n7/suppinfo/nphoton.2009.99_S1.html

Supplementary information Movie 1 (580 kB):
http://www.nature.com/nphoton/journal/v3/n7/extref/nphoton.2009.99-s2.avi

Supplementary information Movie 2 (580 kB):
http://www.nature.com/nphoton/journal/v3/n7/extref/nphoton.2009.99-s3.avi

BackPage of Journal Interview
Interview with Carl Brown - Programmable liquid optical interfaces. *Nature Photonics* 3 (7) (2009) 420. DOI:10.1038/nphoton.2009.114.

Nature Photonics spoke to Carl Brown from Nottingham Trent University about the creation of a voltage-programmable liquid-oil surface that can rapidly switch and deflect light beams.

SUPPLEMENTARY INFORMATION (ADDITIONAL DETAILS)

1. Device Configuration – Solid Dielectric

In the work presented in the manuscript two different solid dielectric layers were used directly on top of the electrodes.

The first was a dielectric stack layer consisting of 17 alternating thin film layers of silicon dioxide and titanium dioxide with a total thickness of 1.13 μm. It was designed to specification and deposited by Yorkshire Photonic Technology Limited, Halifax, U.K. The dielectric stack was designed to be transparent at a wavelength of 633 nm and to be strongly reflecting at 543 nm. The wrinkle amplitude was visualised and measured at 633 nm in transmission in the interferometer whilst simultaneously observing the diffraction of light in reflection at 543 nm due to the periodicity of the wrinkle. A device with this type of dielectric stack was used for the measurements shown in figures 2 and 3 of the manuscript. For figure 3 this enabled simultaneous observation of the time dependent diffraction pattern and measurement of the amplitude of the surface wrinkle at the times between the step voltage changes. This allowed us to ensure that a constant wrinkle amplitude of $A = 0.36$ μm was used for the dynamic measurements at the 3 different oil film thicknesses.

The second was a photoresist layer fabricated from a commercial material, SU-8 (SU8 formulated in GBL, chemically amplified epoxy based negative resist. MicroChem Corporation, 1254 Chestnut Street, Newton, MA 02464, USA). Devices with this type of dielectric layer were used for the transmission measurements shown in figures 4 and 5. The processing of this layer has been described in detail in reference [1]. The main steps in the process are: (i) spin coat SU8-10 in a 50% solution of its own developer (spreading stage followed by 2000 r.p.m. for 30 seconds); (ii) soft bake at 65ºC for 1 minute and 95 ºC for 3 minutes; (iii) flood expose to UV at 50 mW cm^{-2} for 6 seconds; (iv) postbake at 65 ºC for 1 minute and 95 ºC for 1 minute; and (v) harden at 175 ºC for 30 minutes.

2. Liquid surface waves created by vibration

The use of diffraction or scattering of light from liquid surface waves created by vibration has been used historically to measure the liquid surface tension of the liquid [2] and more recently to investigate the damping of low frequency surface acoustic waves [3,4]. In comparison to our approach, where the fluid in a wrinkle is static, the fluid is in constant motion and the diffraction pattern, recorded at near grazing incidence depends on the distance from the "exciter" that is used to vibrate the surface of the fluid.

3. Properties of Oils

There are a range of other physical properties that can be selected to optimise device performance; a selection of possible oils and their properties are listed in table 1. To maximise the amplitude of a wrinkle for a given applied voltage requires a high dielectric constant and low surface tension. However, for a sinusoidal phase profile the intensity of a transmitted zero order is reduced to zero when the difference between the maximum (peak) and the minimum (trough) phase is given by $1.53\pi = 4.80$ radians (from the Fraunhofer approximation for a thin sinusoidal phase grating [5]). To achieve this at a lower wrinkle amplitude, and therefore also at a lower voltage, requires high refractive index oils. In addition, for fast switching response to step changes in the applied voltage a low viscosity is required. There is a compromise in selecting an

oil that has the optimum combination of physical properties, is colourless (at the wavelength used), does not evaporate too quickly, and is non-toxic. From table 1, 1-decanol is a good compromise in this respect. If the commercial RI matching oils are polar and have dielectric constants that are bigger that the square of the refractive index (due to Langevin type contributions) then they are likely to be promising, but at restricted wavelengths because they have some coloration.

4. Extending to Two-Fluid Systems

Our devices involve producing a surface wrinkle on the oil-air interface of a single layer of oil. Such liquid based devices are restricted in their orientation of operation by gravity. However, it is possible that the surface wrinkle could be produced at the interface between two density matched liquids, e.g. oil-water, in an encapsulated device [6]. This type of approach is used in the Varioptic variable focus liquid lens to produce devices which can be used in any orientation and which are robust to shock and mechanical vibrations [7,8]. The disadvantage of this approach is that there is a smaller difference between the refractive indices of oil and water relative to the large difference between the refractive indices of oil and air. Therefore to produce the maximum diffraction efficiency (e.g. to reach the minimum in the transmission of the zero order undeviated beam) the wrinkle amplitude at an oil-water interface would need to be several times larger than the amplitude that would be required at the oil-air interface. Many oils have quite different refractive index to water, but are very similar in density (Table 1).

5. Scaling Results for Equation 1

Equation 1 provides a scaling relationship for the amplitude of a periodic wrinkle to the voltage, V_o, and the film thickness-to-pitch ratio ($\bar{h}/p$) in the form,

$$A = \left(\frac{\alpha(\varepsilon_{oil} - \varepsilon_{air})}{\gamma} \right) V_O^2 \exp\left(-\frac{\beta \bar{h}}{p} \right) \qquad \text{(S1)}$$

This equation was derived for an applied voltage on a film of oil directly on top of the electrodes by considering the change in the dielectric energy stored in the liquid and the interfacial energy stored in an assumed sinusoidal wrinkle of the liquid-air interface above the electrodes and minimising with respect to the wrinkle amplitude. The assumptions in deriving eq. (S1) are,

(i) the wrinkle amplitude is small ($A << p$)
(ii) the periodic potential profile due to the electrodes, $V(x, y)$, is described by a Fourier series expansion to second order only
(iii) the potential profile is unperturbed by the presence of the oil/air interface
(iv) the oil-air interface for a wrinkle is sinusoidal.

For a given electrode width and gap, a Fourier series expansion of the voltage profile can be made and the dielectric energy calculated [9]. To obtain an analytically tractable result this was used in the calculation of the dielectric energy $W_E = \frac{1}{2}\mathbf{D}\cdot\mathbf{E}$, terms to second order were retained, and the energy was then integrated over the fluid volume above the electrodes. The integral involves a series expansion for the case where the wrinkle amplitude is much less than the electrode and gap widths. The net result is an energy that depends on V_o^2, multiplying terms involving a factor with the wrinkle amplitude, and exponentials containing wrinkle amplitude to

pitch (we used equal mark-space ratio). The wrinkling of the liquid-air interface changes its area and this can be calculated for small amplitudes. The combination of these two energies was then minimized with respect to changes in wrinkle amplitude.

6. Validity of Equation S1

Equation S1 provides good design insight into the various physical properties needed to achieve the photonic effects, but experimentally we found a need for a calibration factor in the exponential. The theory has a number of approximations (as described above) to keep it analytically tractable and produce a formula with the key dependencies correctly described (in terms of confirmation by experiment). The number of Fourier modes is truncated and the complexities introduced by the dielectric layer and the distortion in electric field at the upper liquid-air boundary are not accounted for. In addition, the experimental configuration for the devices reported includes a thin dielectric layer between the plane containing the electrodes and the liquid; a complete theoretical treatment would require corrections to the theory described above. However, we have extensive data on decanol testing the scaling laws and further theory and the data, once we have a range of liquids, will form the basis of a subsequent report. For decanol, the experiments have included multiple electrode pitches (40, 80, 120 and 180 μm) and oil film thicknesses between 9.8 μm and 25.1 μm. We have so far found the following experimental scaling relationship holds for a range of values of the oil film height h and pitch, $p=2d$:

$$\log_e\left(\frac{A}{V_o^2}\right) = 6.34 + 2.705\left(\frac{\bar{h}}{d}\right) \qquad \text{(S2)}$$

The analysis does appear to correctly identify dependences on particular parameters, for example obtaining the ratio of the dielectric constant to the surface tension in the coefficient of proportionality gives intuitive insight into how to increase the wrinkle amplitude for a given voltage. Equation S1 provides design insight into the various physical properties needed to achieve the photonic effects; the need for a calibration factor in the exponential is not a fundamental problem in the photonics concept.

Supplementary Information References

[1] Wells, G.G. & Brown, C.V. Rotatable Liquid Crystal Waveplate. *Journal of Materials Science: Materials in Electronics* **20**, 175-180 (2009)

[2] Weisbuch, G. & Garbay, F. Light Scattering by Surface Tension Waves. *Am. J. Phys.* **47**, 355–356 (1979)

[3] Miao, R., Yang, Z.L., Zhu, J.T. & Shen, C.Y . Visualization of low-frequency liquid surface acoustic waves by means of optical diffraction. *Appl. Phys. Lett.* **80**, 3033-3035 (2002)

[4] Dong, J., Miao, R., Qi, J. & Li, F. Unusual distribution of the diffraction patterns from liquid surface waves. *J. Appl. Phys.* **100**, 033108-033110 (2006)

[5] Goodman, J.W. Introduction to Fourier Optics. 2nd ed. New York: McGraw-Hill, 1996.

[6] Brown, C.V., McHale, G., & Newton, M.I. "*Switchable Phase Grating*" UK Patent GB2422680 27 Jan 2005. Equivalents WO2006079821.

[7] Berge, B. & Peseux, J. Variable focal lens controlled by an external voltage: An application of electrowetting. *Eur. Phys. J.* **E3**, 159-163 (2000).

[8] http://www.varioptic.com

[9] Morgan, H., Izquierdo, A.G., Bakewell, D., Green, N.G., & Ramos, A. The dielectrophoretic and travelling wave forces generated by interdigitated electrode arrays: analytical solution using Fourier series. *J. Phys. D* **34**, 1553-1561 (2001).

Table 1: Physical Properties of a Selection of Candidate Oils

Oil	Dielectric Constant	Viscosity (Ns m^{-2})	Surface Tension (mN m^{-1})	Refractive Index	Density (g cm^{-3})
Hexadecane[(a)]	2.05	0.00303	27.47	1.4345	0.773
1-decanol[(a)]	8.1	0.01130	28.4	1.438	0.830
Glycerol[(a)]	47.2	0.945	63.4	1.473	1.26
Nitrobenzene*[(a)]	34.8	0.00178	43.9	1.55	1.2
PDMS 47V20	2.68[(b)]	0.019[(c)]	20.6[(c)]	1.400[(b)]	0.950[(c)]
PDMS 47V350	2.80[(b)]	0.340[(c)]	21.1[(c)]	1.403[(b)]	0.970[(c)]
Immersion oil[(d)]	N/A	0.10-0.12	N/A	1.515	1.025
RI Matching fluid*[(e)]	N/A	0.015	29	1.460-1.570	0.832
RI matching fluid*[(e)]	N/A	0.085	37	1.570-1.640	1.006

N/A : data is not available for this parameter

(a) Knovel Critical tables, 2nd ed. online (2009).

(b) Bluestar Silicones France SAS, Rhodorsil Oils 47 (http://www.bluestarsilicones.com).

(c) Fanton, X., Cazabat, A.M. & Quéré, D. *Langmuir* **12**, 5875-5880 (1996).

(d) Merck Cat. No. 1.04699 “Immersion oils for microscopy”.

(e) Cargille labs, RI matching liquids series A (http://www.cargile.com/refractivestandards.shml).

*Coloured liquid.